The interaction of photons with the graviton background and cosmological observations

Michael A. Ivanov
Physics Dept.,
Belarus State University of Informatics and Radioelectronics,
6 P. Brovka Street, BY 220027, Minsk, Republic of Belarus.
E-mail: ivanovma@tut.by.

Abstract

In the authors model of low-energy quantum gravity, the gravitational interaction of bodies arises as the effect of screening in a sea of super-strongly interacting gravitons. Newton's constant can be calculated as a statistical parameter of the repeated interaction of bodies with gravitons. Small vacuum effects in the model, caused by a new type of interaction - photon-graviton - may have major implications for cosmology. The ones are reviewed here and compared with cosmological observations; this is a self-review of author's works in this approach. The constancy of the ratio $H(z)/(1+z)$ in this model is consistent with observations of the Hubble parameter $H(z)$. Cosmological redshift is a local quantum effect caused by head-on collisions of photons with gravitons, while the additional dimming of distant objects and diffuse cosmic optical background supposedly detected by the New Horizons mission are due to non-head-on collisions. For very soft radiation, the additional relaxation factor is calculated. Since this factor must have different values for soft and hard radiation, the distance modulus in this model must be a multi-valued function of the redshift. The Hubble tension is discussed in this context. The considered quantum effects are beyond the scope of the standard cosmological model. These small effects can describe cosmological observations in a very elegant and unified manner without dark energy and cosmological expansion. Graviton-graviton interactions can lead to the formation of virtual gravitons with very low mass, which may be candidates for the role of dark matter particles.

Key words: low-energy quantum gravity, superstrongly interacting graviton background, photon-graviton interaction, quantum mechanism of redshifts, diffuse cosmic optical background, cosmology without dark energy

1 Introduction

The idea of the expansion of the universe became the basis of modern cosmology and was deeply embedded in the consciousness of physicists. The current prevailing ΛCDM 'concordance' paradigm [1] is based on the Friedman-Lemaitre-Robertson-Walker (FLRW) metric [2].The need to introduce the epoch of inflation [3], dark matter [4] and dark energy [5, 6, 7] into this model takes it beyond the framework of the general theory of relativity itself. Recent observations of massive $z > 7$ galaxies with the James Webb Space Telescope [8, 9], as well as measurements of baryonic acoustic oscillations by the DESI collaboration [10], which may indicate that the dark energy density changes over time, may lead to further modification of the model.

In alternative cosmological models, known as "tired-light" models, the cosmological redshift is treated as a local effect. Several mechanisms for photon energy loss have been proposed [11, 12]. In [13], the Hamiltonian formulation of general relativity was used to study the interaction of photons and gravitons in the first approximation. It has been shown that only a photon with energy $\gg 10^{28}$ eV can decay into another photon and a graviton; this means that this process cannot explain the redshift as a "tired light" phenomenon. This conclusion cannot be transferred to any model of photon-graviton interaction. To avoid introducing an accelerated expansion of the universe, a hybrid model is proposed in [14]: the redshift is considered as a result of expansion and a local mechanism. The latter is based on the introduction of a non-zero photon mass (less than the experimentally established limit), which can cause an energy exchange with galactic or intergalactic background electromagnetic fields, the existence of which is assumed.

The resonant transformation of gravitons into photons with a stochastic magnetic field of primordial nature is considered in [15]. Such a process could be used for indirect detection of gravitational waves by radio telescopes if the resulting photons have a suitable spectrum. For a similar purpose - to use optical instruments for indirect detection of gravitational waves - the scattering of photons on gravitons in the weak field limit is analyzed in [16]. Both massless and massive gravity are considered. The authors have shown that with such scattering, the polarization of light and helicity can change with a very low probability, which in principle makes it possible to study the passage of gravitational waves through a photon field, but only under the condition of using the amplification of weak scattering amplitudes through suitable pre-selected and post-selected scattering states.

After the first detection of gravitational waves [17], Lorentz violation during the propagation of gravitational waves, which may be caused by space-time foam effects, was discussed in [18]. Using additional observations with the Fermi Gamma-Ray Burst Monitor of a transient source in apparent coincidence, a constraint was obtained on the difference between the speeds of light and gravitational waves: $c_g - c < 10^{-17}c$.

In the model of low-energy quantum gravity by the author [19, 20, 21, 22, 23] the cosmological redshift has namely the quantum and local interpretation. Together with additional dimming of distant objects, it results from scattering of photons on super-strong interacting gravitons of the background. Gravity is considered as the screening effect of bodies in this background having the same temperature as CMB. The theoretical Hubble diagram of the model fits observations very well without dark energy. The Hubble parameter $H(z)$ is a linear function of z that is consistent with observations. These small effects are described here and confronted with cosmological observations.

2 Gravity as a screening effect

My model is based on the assumption that gravity is a purely quantum phenomenon, while geometry is just a language for describing the average behavior of large bodies interacting with a graviton background. The geometric language in this model is limited very far from the Planck scales of energies and distances. The basic assumption of the model is the existence of a background of superstrongly interacting gravitons [24]. The interaction cross section $\sigma(E, \epsilon)$ for head-on collisions of any particle with energy E and a graviton with energy ϵ is defined as:

$$\sigma(E, \epsilon) = D \cdot E \cdot \epsilon. \tag{1}$$

The new dimensional constant D should have the value: $D = 0.795 \cdot 10^{-27} m^2/eV^2$. The screening of the superstrongly interacting graviton background creates for any pair of bodies both an attractive force and a repulsive force due to the graviton pressure. For single gravitons, these forces are approximately balanced, but each of them is much stronger than the Newtonian attractive force. In order for the attraction to exceed the repulsion when the background of gravitons is screened by bodies, paired gravitons are needed, which, upon collision, disintegrate into a pair of single gravitons [20]. It turns out that such pairs can be formed in the process of collisions of photons with gravitons [20, 25]. The inverse-square law of classical gravity describes the fundamental quantum effect of this model. The background temperature T determines the values of Newton's constant and Hubble's constant, so that: $G \sim T^6$ and $H_0 \sim T^5$.The ability to calculate Newton's constant G makes the model in some sense underlying general relativity.

3 The photon-graviton interaction

The postulated existence of a graviton background distinguishes this model from all models based on general relativity. Since the ever-present background of gravitons interacting with photons must be in thermodynamic equilibrium with the cosmic microwave background, and in detail, it follows that these two backgrounds must have not only the same temperatures, but also the same energy spectra. This makes it possible to use the rich information contained in Planck's formula for thermal radiation, as well as the Poisson distribution for a random number of gravitons in the plane wave realization. It is a somewhat strange assumption of this model that single gravitons have spin 1, and only paired gravitons have spin 2. Another difference from the cosmic microwave background is that gravitons are endowed in the model with the ability to interact superstrongly in collisions with any microparticles, including gravitons themselves. At the initial stage of development described here, this model does not yet contain such mathematical attributes as the operators of creation and annihilation of particles, commutation relations etc. Using only Eq. 1, Planck spectrum and conservation laws, expressions are obtained for Hubble's constant, which is not associated in this model with the expansion of the universe, and for the magnitude of the additional attenuation of light from a distant source due to the scattering of some photons in non-head-on collisions with background gravitons.

We are dealing here with a homogeneous, non-expanding Universe in Euclidean space.

3.1 Forehead collisions of photons with gravitons

Taking into account Eq. 1, if the average loss of photon energy $\bar{\epsilon}$ in one act of interaction is relatively small compared to the photon energy E (below it is shown that $\bar{\epsilon} = 8.98 \cdot 0^{-4} eV$ at $T = 2.7K$), then the average loss of photon energy along the path dr will be equal to:

$$dE = -aEdr, \tag{2}$$

where a is a constant. If *the entire* redshift is due to this effect, we must define the constant as $a = H_0/c$, where H_0 is Hubble's constant, c is the speed of light, in order to have the Hubble law for small distances. The photon energy E must depend on the distance from the source r as

$$E(r) = E_0 \exp(-ar), \tag{3}$$

where E_0 is the initial value of the energy. We have for $r(z)$:

$$r(z) = ln(1+z)/a. \tag{4}$$

The following example shows how different this model is from the ΛCDM model. The unusually bright galaxy at $z = 14.44$ [26] would be at a distance of 28.74 light gigayears by this model, more than twice as far as the estimated period since the Big Bang would allow. Equations 2 - 4 are the same as those appearing in other tired light models (compare with [12]).

3.2 Non-forehead collisions with gravitons

The average energy loss of the photon flux along the path dr due to non-head-on collisions with gravitons should be proportional to $badr$, where b is a new constant of the order of 1. These losses are due to the deviation of some of the photons from the source-observer direction.

Let us consider the case of a non-head-on collision of a graviton with a photon, when the latter leaves a photon flux, detectable by a distant observer (assumption of a narrow beam of rays) [20, 27]. Since both particles have speeds c, the cross-section of the interaction, which is "visible" at an angle θ (see Fig. 1), will be equal to $\sigma_0 |\cos\theta|$, if σ_0 is the cross-section due to head-on collisions. The function $|\cos\theta|$ allows us to take into account both the forward and backward hemispheres for incoming gravitons. In addition, the flow of gravitons incident on the selected region (cross-section) depends on the angle θ. For the ratio of flows we have:

$$\Phi(\theta)/\Phi_0 = S_s/\sigma_0,$$

where $\Phi(\theta)$ and Φ_0 are the flows incident on σ_0 at an angle θ and perpendicular to it, S_s is the area of the lateral surface of a truncated cone with a base σ_0 (see Fig. 1).

Finally, for the factor b we get [20, 27]:

$$b = 2\int_0^{\pi/2} \cos\theta \cdot (S_s/\sigma_0)\frac{d\theta}{\pi/2}. \tag{5}$$

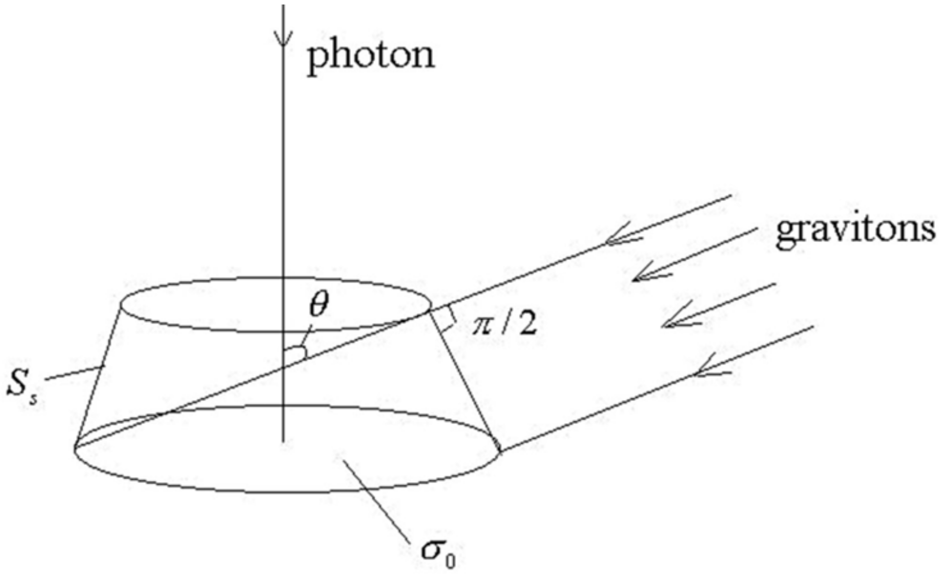

Figure 1: In non-frontal collisions of gravitons with a photon, it is necessary to calculate the lateral surface area of the cone, S_s.

For $0 < \theta < \pi/4$, the formed cone contains self-intersections, and we have: $S_s = 2\sigma_0 \cdot \cos\theta$. For $\pi/4 \leq \theta \leq \pi/2$, we have $S_s = 4\sigma_0 \cdot \sin^2\theta\cos\theta$.

After calculating simple integrals we obtain:

$$b = \frac{4}{\pi}(\int_0^{\pi/4} 2\cos^2\theta d\theta + \int_{\pi/4}^{\pi/2} \sin^2 2\theta d\theta) = \frac{3}{2} + \frac{2}{\pi} \simeq 2.137. \quad (6)$$

Both the redshift and the additional relaxation of any photon flux due to non-frontal collisions of gravitons with photons lead in the model to the following luminosity distance $D_L(z)$:

$$D_L(z) = a^{-1}\ln(1+z) \cdot (1+z)^{(1+b)/2}. \quad (7)$$

3.3 Computation of the Hubble constant

We will assume that the total redshift is caused by interactions with single gravitons [20, 25]. If $\sigma(E,\epsilon)$ is the cross section of head-on collisions of a photon with energy E with a graviton with energy ϵ, we actually assume (see Eq. 1) that

$$\frac{d\sigma(E,\epsilon)}{Ed\Omega} = const(E),$$

where $d\Omega$ is the element of the spatial angle, and the function $const(x)$ has a constant value for any x. If $f(\omega,T)d\Omega/2\pi$ is the spectral density of the graviton flux within $d\Omega$ in some direction (ω is the graviton frequency, $\epsilon = \hbar\omega$), i.e. the intensity of the graviton flux is equal to the integral $(d\Omega/2\pi)\int_0^\infty f(\omega,T)d\omega$, where T is the equivalent temperature of the graviton background, then for the Hubble constant we can write:

$$H_0 = \frac{1}{2\pi}\int_0^\infty \frac{\sigma(E,\epsilon)}{E} f(\omega,T)d\omega.$$

If $f(\omega, T)$ is described by Planck's formula for equilibrium radiation, then

$$\int_0^\infty f(\omega, T) d\omega = \sigma T^4,$$

where σ is the Stefan-Boltzmann constant. Using eq. 1, we then obtain:

$$H_0 = \frac{1}{2\pi} D \cdot \bar{\epsilon} \cdot (\sigma T^4) = \frac{15 D k \sigma T^5}{2\pi^5} I_4, \tag{8}$$

where $\bar{\epsilon}$ is the average energy of a graviton:

$$\bar{\epsilon} \equiv \int_0^\infty \hbar\omega \cdot \frac{f(\omega, T)}{\sigma T^4} d\omega = \frac{15}{\pi^4} I_4 k T, \tag{9}$$

where

$$I_4 \equiv \int_0^\infty \frac{x^4 dx}{\exp(x) - 1} = 24.866.$$

Since $\bar{\epsilon} = 8.98 \cdot 10^{-4} eV$ at $T = 2.7K$, we obtain the following theoretical value of the Hubble constant: $H_0 = 2.14 \cdot 10^{-18}\ s^{-1} \equiv 66.875\ km \cdot s^{-1} \cdot Mpc^{-1}$.

The resulting formula for the Hubble constant remains valid for the case when some of the background gravitons are paired [20]: a twofold increase in the energy of paired gravitons is accompanied by a twofold decrease in the number of such gravitons compared to the number of single gravitons participating in the pairing, so the average energy of gravitons does not change.

4 The Hubble parameter $H(z)$ of this model

The photon energy losses due to head-on collisions with background gravitons alone yield a geometric distance/redshift relationship of Eq. 7. Then the Hubble parameter $H(z)$ in this model can be defined as [20]:

$$H(z) \equiv \frac{dz}{dr} \cdot c = H_0 \cdot (1 + z). \tag{10}$$

It means that in the model:

$$\frac{H(z)}{(1 + z)} = H_0. \tag{11}$$

The last formula gives us the possibility to evaluate the Hubble constant using observed values of the Hubble parameter $H(z)$. The weighted average value of the Hubble constant may be calculated by the formula:

$$< H_0 >= \frac{\sum \frac{H(z_i)}{1+z_i} / \sigma_i^2}{\sum 1/\sigma_i^2}. \tag{12}$$

The weighted dispersion of the Hubble constant may be found with the same weights:

$$\sigma_0^2 = \frac{\sum (\frac{H(z_i)}{1+z_i} - < H_0 >)^2 / \sigma_i^2}{\sum 1/\sigma_i^2}. \tag{13}$$

The χ^2 value is calculated as:

$$\chi^2 = \sum \frac{(\frac{H(z_i)}{1+z_i} - < H_0 >)^2}{\sigma_i^2}. \tag{14}$$

Then we have [20] for the data set of observed values of the Hubble parameter $H(z)$ (40 points) of [31]: $< H_0 > \pm\sigma_0 = (60.566 \pm 3.513)\ km \cdot s^{-1} \cdot Mpc^{-1}$. The value of χ^2 is now equal to 32.529. By 40 degrees of freedom of this data set, it means that the hypothesis described by Eq. (11) cannot be rejected with 79.33% C.L. The weighted average value of the Hubble constant with $\pm\sigma_0$ error bars are shown in Fig. 2 as horizontal lines; observed values of the ratio $H(z)/(1+z)$ with $\pm\sigma_i/(1+z)$ error bars are shown in Fig. 2, too (points).

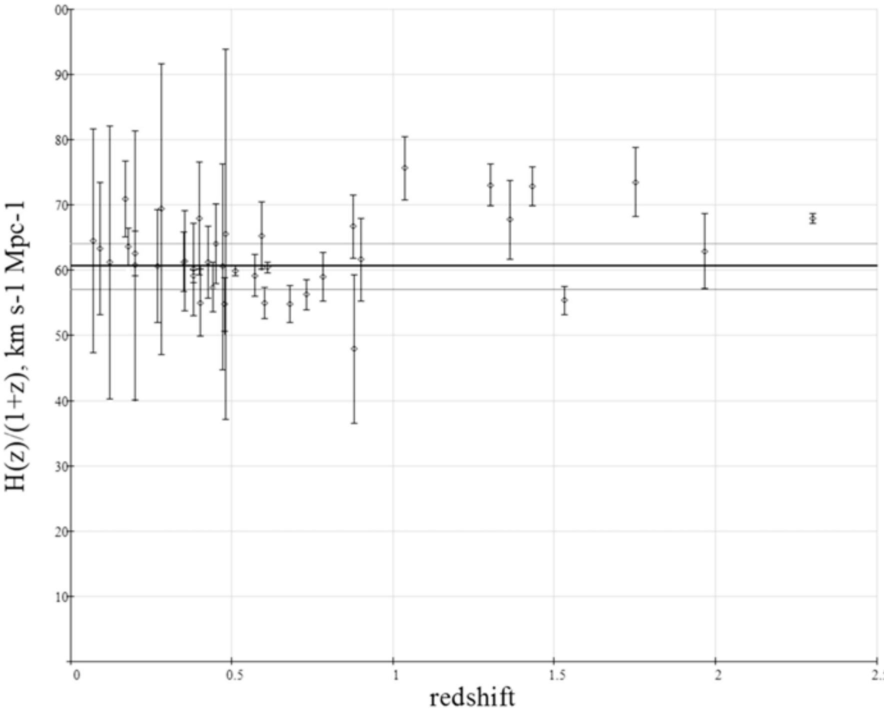

Figure 2: The ratio $H(z_i)/(1+z_i) \pm \sigma_{0i}$ and the weighted value of the Hubble constant $< H_0 > \pm\sigma_0$ (horizontal lines). Observed values of the Hubble parameter $H(z_i)$ (40 points) are taken from Table 1 of [31].

The $R_h = ct$ cosmological model (a Friedmann-Robertson-Walker cosmology with zero active mass) has the same function $H(z)$ as the considered one; R_h is the Hubble radius.

5 The volume/redshift relation

The geometrical distance/redshift relation of this model: $r(z) = ln(1+z) \cdot c/H_0$, leads to the volume/redshift relation [32]:

$$V(z) = 4/3 \cdot \pi(ln(1+z) \cdot c/H_0)^3 \equiv A \cdot (ln(1+z))^3, \quad (15)$$

where $A \equiv 4/3 \cdot \pi(c/H_0)^3 = 13627$ Gyr^3 by the theoretical value of H_0 in the model: $H_0 = 2.14 \cdot 10^{-18}\ s^{-1} = 66.875\ km \cdot s^{-1} \cdot Mpc^{-1}$. The derivative of this function is equal to:

$$\frac{dV}{dz} = \frac{3A}{1+z} \cdot (ln(1+z))^2. \tag{16}$$

Its graph is shown in Fig. 3. The derivative has a maximum near $z = 6.4$, and further it decreases more than 2.5 times up to $z = 100$. An observer may conclude that the universe becomes more and more empty by $z > 6.4$, if a concentration of galaxies remains really constant.

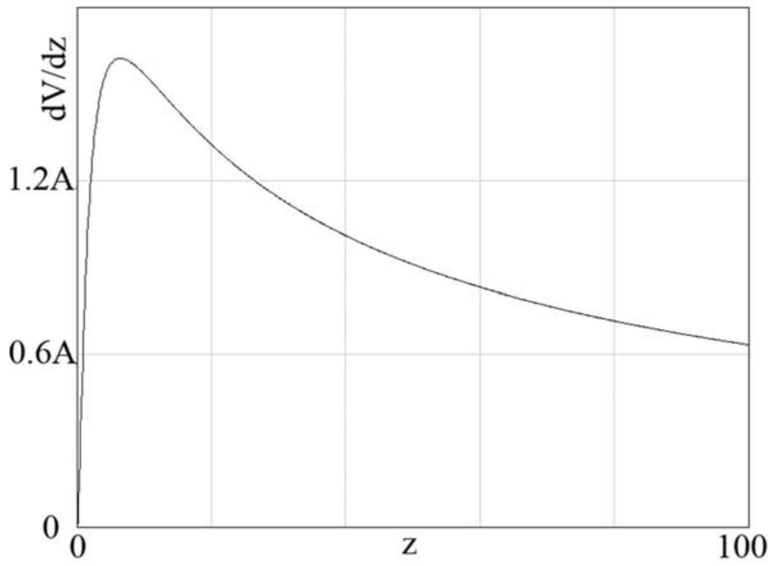

Figure 3: The graph of derivative $\frac{dV}{dz}$ for a big range of z [32].

6 The Hubble diagram of this model

Both forehead and non-forehead collisions with gravitons give the luminosity distance/redshift relation of Eq. 7, where the parameter b belongs to the range 0 - 2.137 ($b = \frac{3}{2} + \frac{2}{\pi} \simeq 2.137$ for very soft radiation, and $b \to 0$ for very hard one). Because of this, the distance modulus should be a multivalued function of the redshift [20]: for a given z, b may have different values for different kinds of sources. To fit this model, observations should be corrected for no time dilation as: $\mu(z) \to \mu(z) + 2.5 \cdot \lg(1+z)$, where $\lg x \equiv \log_{10} x$, and the distance modulus: $\mu(z) \equiv 5lgD_L(z)(Mpc) + 25$.

The graphs of theoretical distance moduli $\mu(b,z)$ for $b = 2.137$ and $b = 0$ (with the correction for the effect of time dilation of the standard model: $b \to b-1$) are shown in Fig. 4 [33]; for comparison, the graph of $\mu_c(z)$ for the flat Universe with the concordance cosmology by $\Omega_M = 0.3$ and $w = -1$ is shown, too. Possibly, positive low redshift values of the difference $\mu_c(z) - \mu(2.137, z)$ can be related to the Hubble tension in LCDM cosmology [28, 29, 30] if the function $\mu(2.137, z)$ describes the observations better. The maximum difference between $\mu_c(z)$ and $\mu(2.137, z)$ for $z \leq 10$ is equal to -0.54, it increases up to -0.87 for $z \leq 20$.

Data set	b	χ^2	C.L., %	$< H_0 > \pm\sigma_0$
SCP Union 2.1 [37]	2.137	239.635	100	68.22 ± 6.10
JLA [34]	2.365	30.71	43.03	69.54 ± 1.58
109 long GRBs [38]	2.137	70.39	99.81	66.71 ± 8.45
44 long GRBs [39],	2.137	40.585	57.66	69.73 ± 37.23
the Amati calibration	**1.885**	39.92	60.57	60.31 ± 31.93
44 long GRBs [39],	2.137	43.148	46.5	70.39 ± 38.79
the Yonetoku calibration	**1.11**	32.58	87.62	38.84 ± 18.55
quasars [40]	2.137	23.378	13.73	69.53 ± 10.87

Table 1: Results of fitting the Hubble diagram with the model of low-energy quantum gravity[35]. The best fitting values of b for 44 long GRBs are marked by the bold typeface.

Since $D_L(z)$ in Eq. 7 is proportional to $1/H_0$, the possible dependence $b(z)$ due to the change in the frequency of light on its way from the source to the observer may be another cause of the Hubble tension. The function $b(z)$ should increase with increasing z, so the decrease of $D_L(z)$ by $z \to 0$ in this model can be interpreted in the standard model as an increase of H_0 at small z.

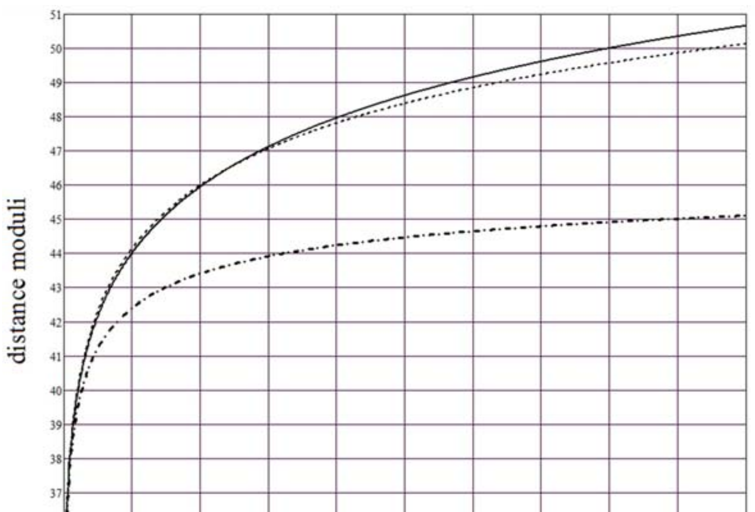

Figure 4: Three theoretical Hubble diagrams [33]: $\mu(b, z)$ of this model with $b = 2.137 - 1$ (solid) and $b = 0 - 1$ (dash-dot) to take into account the effect of time dilation of the standard model; and for comparison, $\mu_c(z)$ for the flat Universe with the concordance cosmology by $\Omega_M = 0.3$ and $w = -1$ (dash).

Using SN 1a observations from the SCP Union 2.1 compilation (580 supernovae) [37], the theoretical Hubble diagram $\mu_0(z)$ of this model with $b = 2.137$ was fitted to observations with H_0 as a free parameter [35]. Results are shown in Fig. 5; the value of Hubble's constant from the fitting is:

$$< H_0 > \pm\sigma_0 = (68.223 \pm 6.097) km/s \cdot Mpc.$$

Given $H_0 =< H_0 >$, we get $\chi^2 = 239.63$ that gives C.L. of 100%. If we divide this data set into two subsets: the first with $z < 0.150$ and the second with $z > 0.150$, we can see the manifestation of the Hubble tension in this model at constant $b = 2.137$, although with great uncertainty. For the first subset we obtain an estimate of the Hubble constant: $< H_0 > \pm\sigma_0 = (69.411 \pm 5.402) km/s \cdot Mpc$, and for the second: $< H_0 > \pm\sigma_0 = (65.710 \pm 5.391) km/s \cdot Mpc$.

I have used [22] 31 binned points of the JLA compilation from Tables F.1 and F.2 of [34] (diagonal elements of the correlation matrix in Table F.2 are dispersions of distance moduli). Varying the value of b, we find the best fitting value of this parameter: $b = 2.365$ with $\chi^2 = 30.71$. It means that the best fitting has 43.03% C.L. This value of b is 1.107 times greater than the theoretical one. For the Hubble constant we have in this case: $< H_0 > \pm\sigma_0 = (69.54 \pm 1.58)\ km \cdot s^{-1} \cdot Mpc^{-1}$.

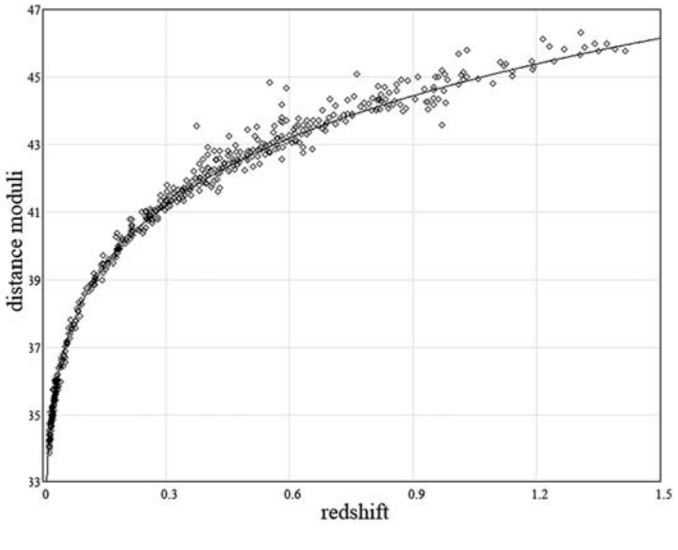

Figure 5: The theoretical Hubble diagram $\mu_0(z)$ of this model (solid); Supernovae 1a observational data (580 points of the SCP Union 2.1 compilation) are taken from [37] and corrected for no time dilation.

In my paper [35] results of fitting the Hubble diagram for different data sets of remote objects with the model of low-energy quantum gravity are summarized in Table 1; its part is shown here as Table 1. For best fitting values of b in a case of 44 long GRBs, values of distance moduli are overestimated in both calibrations: on ~ 0.225 for the Amati calibration, and on ~ 1.18 for the Yonetoku calibration. It leads to the corresponding underestimation of the Hubble constant. The theoretical Hubble diagram of the model should be the multivalued function of the redshift for soft and hard radiations; perhaps, this feature may be seen for the 44 GRBs data set with the Yonetoku calibration [23]. GRB observational data with the Yonetoku calibration (44 points) were taken from Table 3 of [39] and corrected for no time dilation. Another set of

GRB observational data, which for small z are calibrated using SNe 1a with the Amati calibration, (109 points) was taken from Tables 1,2 of [38], corrected for no time dilation and fitted in the same manner with $b = 2.137$ [20]. In this case we have $\chi^2 = 70.39$ that corresponds to 99.81% CL of fitting (see Fig. 6).

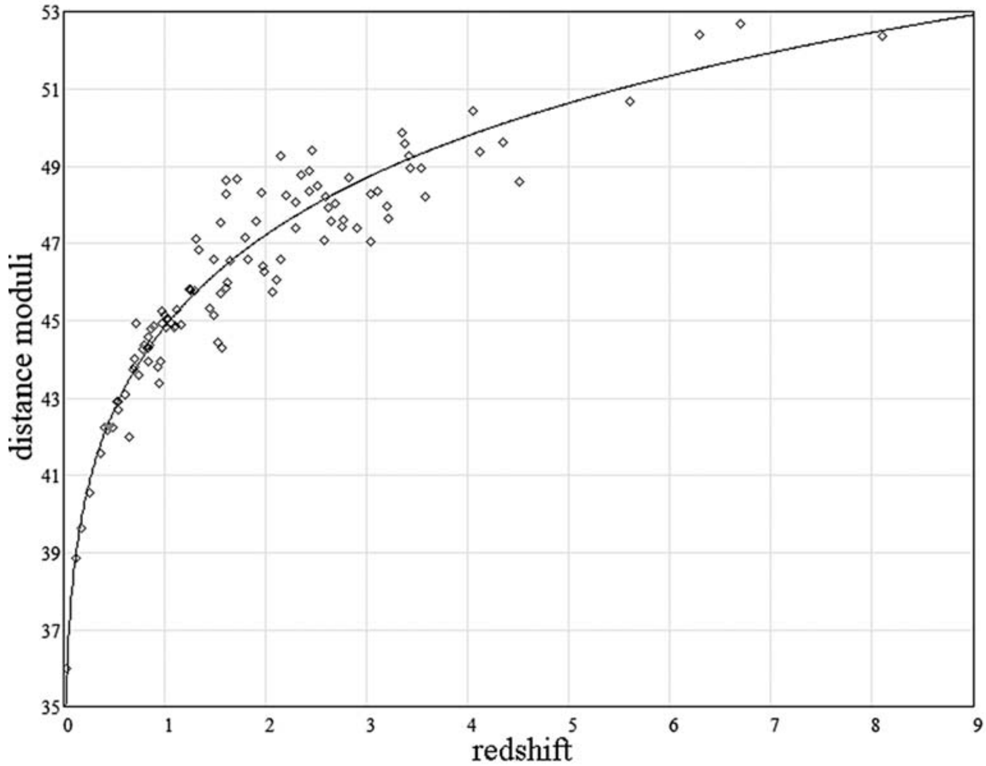

Figure 6: The theoretical Hubble diagram $\mu_0(z)$ of this model (solid); long GRBs observational data with the Amati calibration (109 points) are taken from Tables 1,2 of [38] and corrected for no time dilation.

In this model, the functions $r(z)$ and $D_L(z)$ are found at present for radiation consisting of photons with energies $\hbar\omega \gg \bar{\epsilon}$, where $\bar{\epsilon}$ is the average graviton energy. But for $\hbar\omega \ll \bar{\epsilon}$, e.g. for the radio band, the situation is more complicated [22]. In this case, only a small part of the background gravitons will transfer their momentum to photons in head-on collisions, and this momentum will often be of the same order as the photons' own momentum. This should lead to a large broadening of the emission spectrum towards the red, and its redshift as a whole will be much smaller than expected for high-energy radiation. From another side [22], all gravitons with energies $\epsilon > \hbar\omega$ are able to get the photon momentum in such the collisions that should additionally attenuate the radiation flux. This means that the known redshift z and the constant parameter b are not enough to describe the situation; this issue remains open. This feature of the model may be important for measurements of the redshifted 21-cm radiation, which are now of great interest [41, 42, 43], and fast radio bursts (FRBs) to understand their origin and large dispersive delays [44, 45, 46].

7 The light from nowhere effect

After non-forehead collisions, scattered photons should create the light from nowhere effect which has not an analog in the standard cosmological model [47]. The scattered photons will be redshifted proportionally to passed random distances. Because of this randomness of angles of scattering and passed distances, it is difficult to compute the sky brightness in the optical range, for example, due to this light from nowhere effect. It is necessary to know the ratio $\delta(z)$ of the scattered flux to the the remainder $\Phi(z) \equiv L/D_L^2(b,z)$ reaching the observer, and, at least, the light flux of galaxies and their number counts by different redshifts. To evaluate how big is the ratio $\delta(z)$, we can compute the flux $\Phi_0(z) \equiv L/D_L^2(0,z)$, where L is the luminosity, $D_L(b,z)$ and $D_L(0,z)$ are luminosity distances by $b \neq 0$ and $b = 0$. $\Phi_0(z)$ corresponds to the absence of non-forehead collisions. Then the ratio may be defined as:

$$\delta(z) \equiv (\Phi_0(z) - \Phi(z))/\Phi(z). \tag{17}$$

Using $Eq.$ 10 we get:

$$\delta(z) = (1+z)^b - 1. \tag{18}$$

We have by $b = 2.137$: $\delta(0.4) = 1.05$, $\delta(1) = 3.34$, $\delta(2) = 9.46$. But a problem to compute the sky brightness remains open: one should take into account the randomness of angles of scattering and passed distances of photons in some probabilistic manner.

After non-forehead collisions, scattered photons should create the light-from-nowhere effect which has not an analog in the standard cosmological model. The ratio $\delta(z)$ of the scattered flux to the remainder reaching the observer is equal to:

$$\delta(z) = (1+z)^b - 1. \tag{19}$$

By $b = 2.137$ we have, for example: $\delta(0.4) = 1.05$, i.e. this effect is big enough to explain a tentative detection of a diffuse cosmic optical background [36].

8 The galaxy number counts-redshift relation

Total galaxy number counts $dN(r)$ for a volume element $dV = d\Omega r^2 dr$ is equal to: $dN(r) = n_g dV = n_g d\Omega r^2 dr$, where n_g is a galaxy number density (it is constant in the no-evolution scenario), $d\Omega$ is a solid angle element. Using the function $r(z)$ of this model, we can re-write galaxy number counts as a function of a redshift z [20, 21, 35, 48]:

$$dN(z) = n_g d\Omega (H_0/c)^{-3} \frac{ln^2(1+z)}{1+z} dz. \tag{20}$$

Let us introduce a function (see [49]):

$$f_2(z) \equiv \frac{(H_0/c)^3 dN(z)}{n_g d\Omega z^2 dz};$$

then we have for it in this model:

$$f_2(z) = \frac{ln^2(1+z)}{z^2(1+z)}. \tag{21}$$

A graph of this function is shown in Fig. 7; the typical error bar and data point are added here from paper [50] by Loh and Spillar. There is not a visible contradiction with observations. *There is not any free parameter in the model to fit this curve;* it is a very rigid case.

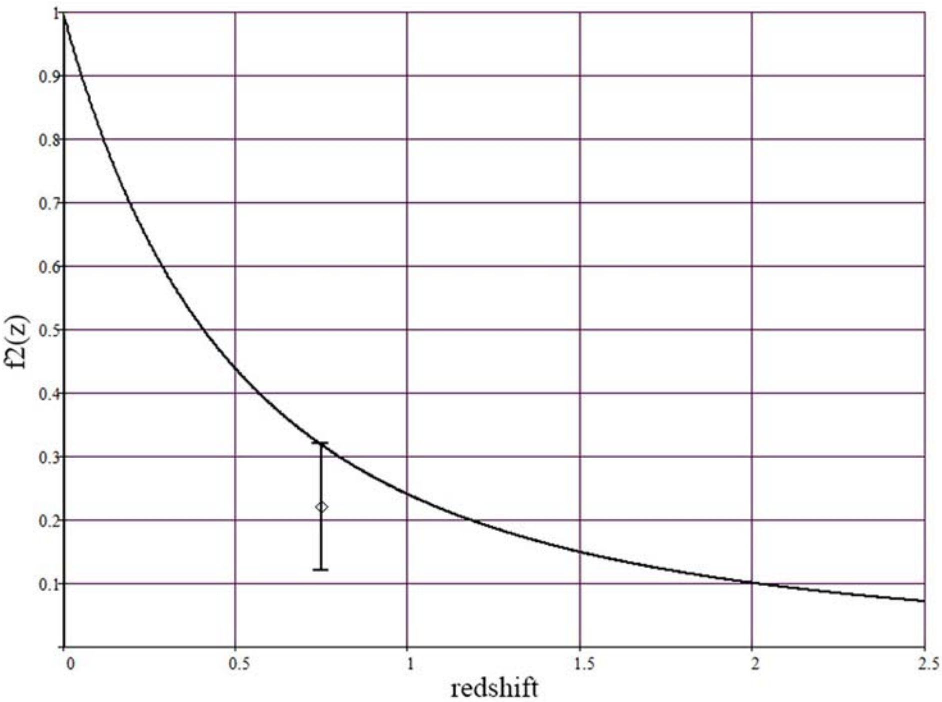

Figure 7: Number counts f_2 as a function of the redshift in this model [21, 48]. The typical error bar and data point are taken from paper [50] by Loh and Spillar.

It is impossible to count a *total* galaxy number for big redshifts so as very faint galaxies are not observable. For objects with a fixed luminosity, it is easy to find how their magnitude m changes with a redshift [21, 48]. So as $dm(z)$ under a constant luminosity is equal to: $dm(z) = 5d(lgD_L(z))$, we have for $\Delta m(z_1, z_2) \equiv \int_{z_1}^{z_2} dm(z)$:

$$\Delta m(z_1, z_2) = 5lg(f_1(z_2)/f_1(z_1)). \tag{22}$$

This function is shown in Fig.8 for $z_1 = 0.001; 0.01; 0.1$.

I would like to note that a very fast *initial* growth of the luminosity distance with a redshift z in this model might explain the observed excess of faint blue galaxy number counts above an expected one in the standard model [48]. A galaxy color depends on a redshift, and a galaxy dimming depends on the luminosity distance, because by big values of the ratio $\Delta m(z_1, z_2)/(z_2 - z_1)$ in a region of small redshifts and by a further much slower change of it (see Fig.9) an observer will see many faint but blue enough galaxies in this region (in the no-evolution scenario) [20].

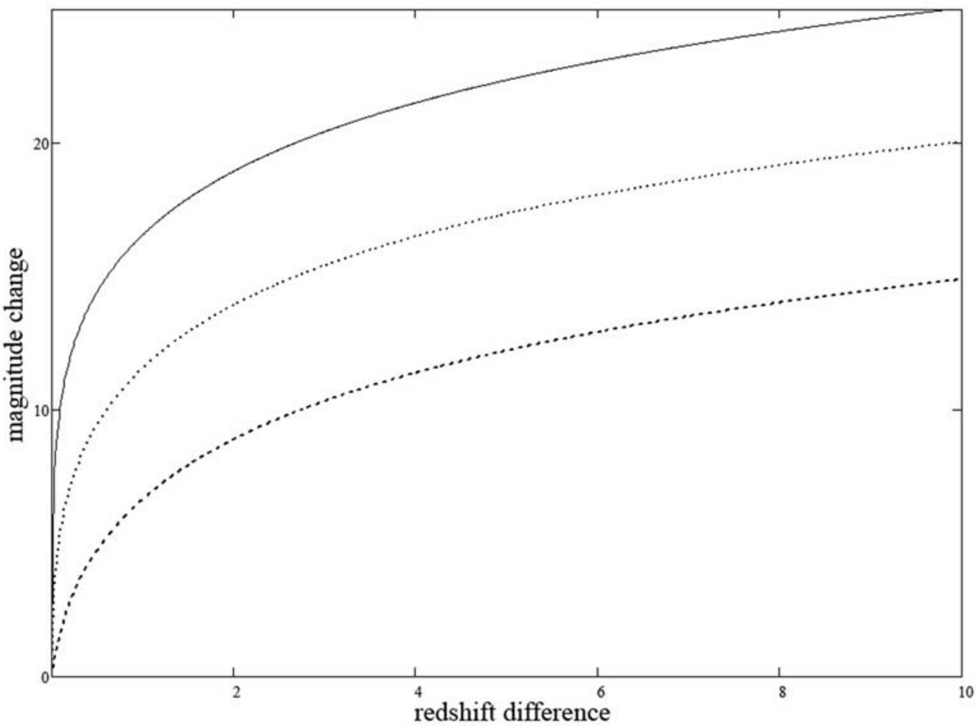

Figure 8: Magnitude changes Δm as a function of the redshift difference $z_2 - z_1$ in this model for $z_1 = 0.001$ (solid); 0.01 (dot); 0.1 (dash) [21, 48].

9 Virtual massive gravitons as dark matter particles

Unlike models of expanding universe, in this model a problem of utilization of energy, lost by radiation of remote objects, exists [20, 21, 35, 47]. A virtual graviton forms under collision of a photon with a graviton of the graviton background. It should be massive if an initial graviton transfers its total momentum to a photon; it follows from the energy conservation law that its energy $\epsilon^{'}$ must be equal to 2ϵ if ϵ is an initial graviton energy. By force of the uncertainty relation, one has for a virtual graviton lifetime $\tau : \tau \leq \frac{\hbar}{\epsilon^{'}}$, i.e. for $\epsilon^{'} \sim 10^{-3} eV$ it is $\tau \leq 10^{-12} s$. By force of conservation laws for energy, momentum and angular momentum, the virtual graviton may decay into no less than three real gravitons [22]. In a case of decay into three gravitons, their energies should be equal to $\epsilon, \epsilon^{''}, \epsilon'''$, with $\epsilon^{''} + \epsilon''' = \epsilon$. So, after this decay, two new gravitons with $\epsilon^{''}, \epsilon''' < \epsilon$ inflow into the graviton background. It is a source of refilling the graviton background. Collisions of gravitons with massive bodies, leading to their deceleration, should provide the bulk of this replenishment.

From another side [22], a self-interaction of gravitons of the background should also lead to the formation of virtual massive gravitons with energies less than ϵ_{min} where ϵ_{min} is a minimal energy of gravitons of an interacting pair. If gravitons with energies $\epsilon^{''}, \epsilon'''$ experience a series of collisions with gravitons of

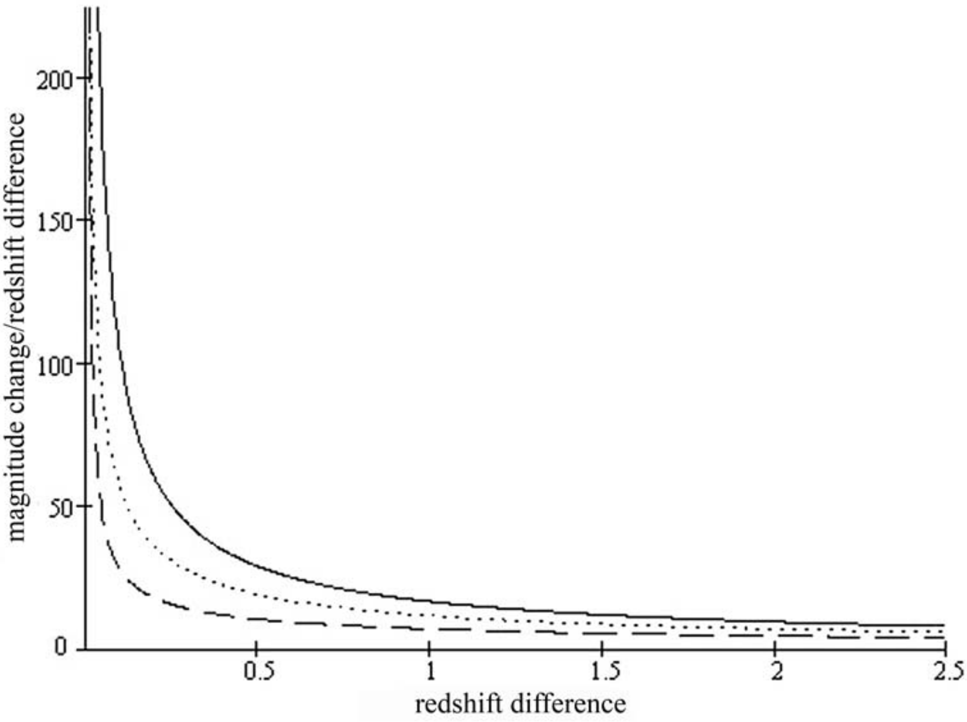

Figure 9: To a possible explanation of the excess of faint blue galaxy number counts [48]: $\Delta m(z_1, z_2)/(z_2 - z_1)$ vs. the redshift difference $z_2 - z_1$ in this model for $z_1 = 0.001$ (solid); 0.01 (dot); 0.1 (dash).

the background, their lifetime should increase. In every such a cycle collision-decay, an average energy of "redundant" gravitons will double decrease, and its lifetime will double or more increase. Only for ~ 93 cycles, a lifetime will have increased from $10^{-12}s$ to as minimum 1 Gyr. Such virtual massive gravitons, with the lifetime increasing from one collision to another, would be ideal dark matter particles. The ones will not interact with matter in any manner except usual gravitation. The ultracold gas of such gravitons will condense under the influence of gravitational attraction. In addition, even in the absence of the initial inhomogeneity in such the gas, it will easily arise. It is a way of cooling the graviton background.

The model of the composite fundamental fermions by the author [51] has all symmetries of the standard model of elementary particles on global level. Possibly virtual gravitons with very low masses are quite acceptable for the role of components of such the fermions.

10 How to verify the quantum redshift mechanism

The main conjecture of this approach about the quantum nature of redshifts may be verified in a ground-based laser experiment. To do it, one should compare spectra of laser radiation before and after passing some distance l in a high-vacuum tube [20, 21, 35]. The temperature T of the graviton background coincides in the model with the one of CMB. Assuming $T = 2.7K$, we have for the average graviton energy: $\bar{\epsilon} = 8.98 \cdot 10^{-4}$ eV. Because of the quantum nature of redshift, the satellite of main laser line of frequency ν would appear after passing the tube with a redshift of 10^{-3} eV/h, and its position should be fixed. It will be caused by the fact that on a very small way in the tube only a small part of photons may collide with gravitons of the background. The rest of them will have unchanged energies. The center-of-mass of laser radiation spectrum should be shifted proportionally to a photon path. Due to the quantum nature of shifting process, the ratio of satellite's intensity to main line's intensity should have the order: $\sim \frac{h\nu}{\bar{\epsilon}} \frac{H_0}{c} l$. Given a very low signal photon number frequency, one could use a single photon counter to measure the intensity of the satellite line after a narrow-band filter with filter's transmittance k. If q is a quantum output of a photomultiplier cathode, f_n is a frequency of its noise pulses, and n is a desired signal-to-noise ratio, then an evaluated time duration t of data acquisition would be equal to:

$$t = \frac{(\bar{\epsilon} c n)^2 f_n}{(H_0 q k P l)^2}, \tag{23}$$

where P is a laser power. Assuming for example: $n = 10$, $f_n = 10^3$ s^{-1}, $q = 0.3$, $k = 0.1$, $P = 200$ W, $l = 300$ km, we have the estimate: $t \approx 3 \cdot 10^3$ s. Such the value of l may be achieved if one forces a laser beam to whipsaw many times between mirrors in the vacuum tube with the length of a few kilometers.

The advanced *LIGO* detectors [52, 53] have many technological achievements needed to do the described experiment: stable powerful lasers and input optics, high-vacuum tubes with optical resonator that multiplies the physical length by the number of round-trips of the light, mirror suspension systems with actuators. Some parameters of *LIGO* systems are of the same order as in the considered example. If one constructs a future *LIGO* detector with some additional equipment, the verification of the redshift mechanism may be performed in parallel with the main task or during a calibration stage of the detector.

11 Conclusion

The considered quantum effects are beyond the scope of the standard cosmological model. These small effects can describe cosmological observations in a very elegant and unified manner without dark energy and cosmological expansion [20, 54]. It is perhaps a paradoxical coincidence that the desire of cosmologists to find new physics, and the long-standing expectation of high-energy physicists and gravitational scientists to discover some quantum gravity effect will be satisfied by recognizing the century-old redshift as a local quantum effect. If the discovery of a diffuse cosmic optical background by the New Horizons mission [36] is confirm by future missions, it will be a big puzzle for the standard cosmological model. The described possibility of interpreting dark matter as a gas of virtual massive gravitons, which cannot be detected, but can be the foremother for all visible matter, seems attractive.

The presented analysis of the interaction of photons with the graviton background is currently incomplete, since it does not contain an important fragment

- an analysis of the deflection of photons when they pass near massive bodies. When calculating the factor b in the article, the probability of a photon deviation from its original direction of propagation in an isotropic background of gravitons was calculated. However, near a massive body, it will be necessary to take into account the background anisotropy caused by the scattering of gravitons by the body. Another unsolved problem is the calculation of the attenuation factor b for an arbitrary photon energy; so far it has been found only for very soft and very hard radiation. The solution to this problem would allow, in particular, to describe the dependence of the factor b on the redshift z. This would allow the model to describe in detail the effect of decreasing $b(z)$ at lower redshifts, which in the ΛCDM model is known as the Hubble tension (or crisis).

Data Availability Statement

The data used in this study are publicly available and taken from the cited articles.

References

[1] Lahav, O., Liddle, A.R. The Cosmological Parameters (2021). The Review of Particle Physics 2022 (aka the Particle Data Book), Oxford University Press, 467-475, (2022) https://doi.org/10.48550/arXiv.2201.08666

[2] Melia, F. The Friedmann-Lemaitre-Robertson-Walker metric. Mod. Phys. Lett. A **37**(3), 2250016 (2022) https://doi.org/10.1142/S021773232250016X

[3] Liu, J., Melia, F. Challenges to Inflation in the Post-Planck Era. Astrophys. J. **967**, 109 (2024) https://doi.org/10.3847/1538-4357/ad4036

[4] Oks, E. Brief Review of Recent Advances in Understanding Dark Matter and Dark Energy. New Astron. Rev. **93**, 101632 (2021) https://doi.org/10.1016/j.newar.2021.101632

[5] Carfora, M., Familiari, F. How Dark is Dark Energy?. arXiv:2401.04293 [astro-ph.CO] (2024) https://doi.org/10.48550/arXiv.2401.04293

[6] Zhang, R., Zhang, Z. Dark Energy on Astrophysical Scales and Its Detection in the Milky Way. JCAP **06**, 031 (2023) https://doi.org/10.1088/1475-7516/2023/06/031

[7] Wang, B, Abdalla, E., Atrio-Barandela, F., Pavon, D. Further understanding the interaction between dark energy and dark matter: current status and future directions. arXiv:2402.00819 [astro-ph.CO] (2024) https://doi.org/10.48550/arXiv.2402.00819

[8] Boylan-Kolchin, M. Stress testing ΛCDM with high-redshift galaxy candidates. Nature Astron. **7**, 731-735 (2023) https://doi.org/10.1038/s41550-023-01937-7

[9] Glazebrook, K., Nanayakkara, T., Schreiber C. et al. A massive galaxy that formed its stars at $z \approx 11$. Nature **628**, 277-281(2024) https://doi.org/10.1038/s41586-024-07191-9

[10] DESI Collaboration: Adame, A. G., Aguilar, J., Ahlen, S., Alam, S. et al. DESI 2024 VI: Cosmological Constraints from the Measurements of Baryon Acoustic Oscillations. arXiv:2404.03002v3 [astro-ph.CO] (2024) https://doi.org/10.48550/arXiv.2404.03002

[11] Zwicky, F. On the Red Shift of Spectral Lines through Interstellar Space. Proc. Nat. Acad. Sci. **15**, 773-779 (1929) https://doi.org/10.1073/pnas.15.10.773

[12] LaViolette, P.A. Is the Universe Really Expanding?. Astrophys. J. **301**, 544 (1986) https://doi.org/10.1086/163922

[13] Weber, J., Hinds, G. Interaction of Photons and Gravitons. Phys. Rev. **128**, 2414 (1962) https://doi.org/10.1103/PhysRev.128.2414

[14] Spallicci, A.D.A.M., Sarracino, G., Capozziello, S. Investigating dark energy by electromagnetic frequency shifts. Eur. Phys. J. Plus **137**, 253 (2022) https://doi.org/10.1140/epjp/s13360-022-02450-y

[15] Addazi, A., Capozziello, S., Gan, Q. Resonant Graviton-Photon Conversion with Stochastic Magnetic Field in the Expanding Universe. arXiv:2401.15965 [gr-qc] (2024) https://doi.org/10.48550/arXiv.2401.15965

[16] Athira, B. S., Mandal, S., Banerjee, S. Characteristics of interaction between Gravitons and Photons. Eur. Phys. J. Plus **136**, 403 (2021) https://doi.org/10.1140/epjp/s13360-021-01361-8

[17] Abbott, B.P., Abbott, R., Abbott, T.D., Abernathy, M.R., Acernese, F., Ackley, K., Adams, C., Adams, T., Addesso, P. et al. (LIGO Scientific Collaboration and Virgo Collaboration). Observation of Gravitational Waves from a Binary Black Hole Merger. Phys. Rev. Lett. **116**(6), 061102 (2016) https://doi.org/10.1103/PhysRevLett.116.061102

[18] Ellis, J., Mavromatos, N.E., Nanopoulos, D.V. Comments on Graviton Propagation in Light of GW150914. Mod. Phys. Lett. A **31**(26), 1650155 (2016) https://doi.org/10.1142/S0217732316750018

[19] Ivanov, M.A. Gravitons as super-strong interacting particles, and low-energy quantum gravity In: D.C. Moore (Ed.), Focus on Quantum Gravity Research, Nova Science, NY, 89-120 (2006) arXiv:hep-th/0506189v3 (2006) https://doi.org/10.48550/arXiv.hep-th/0506189

[20] Ivanov, M.A. Selected papers on low-energy quantum gravity. http://ivanovma.narod.ru/selected-papers-Ivanov2018.pdf (2018)

[21] Ivanov, M.A. Low-energy quantum gravity and cosmology. In: V. Krasnoholovets (Ed.), The origin of gravity from the first principles, Nova Science, NY, 2021, pp 23-56 (2021). https://vixra.org/pdf/2011.0180v2.pdf.

[22] Ivanov, M.A. Superstrongly interacting gravitons: low-energy quantum gravity and vacuum effects. *Horizons in World Physics*. Volume 312; Reimer, A. (Ed.); Nova Science, NY, 2024, pp. 225-240.

[23] Ivanov, M.A. Quantum gravity without quantization. Current Physics **1**, e27723348344123 (2024) https://doi.org/10.2174/0127723348344123241030061731.

[24] Ivanov, M.A. Screening the graviton background, graviton pairing, and Newtonian gravity. arXiv:gr-qc/0207006v3 (2006) https://doi.org/10.48550/arXiv.gr-qc/0207006

[25] Ivanov, M.A. Gravity as a screening effect. Current Physics, in press, e27723348373429. https://doi.org/10.2174/0127723348373429250512104534 Rohan P.

[26] Naidu, R.P,, Oesch, P.A., Brammer, G., Weibel, A. et al. A cosmic miracle: a remarkably luminous galaxy at $z_{spec} = 14.44$ confirmed with JWST. arXiv:2505.11263 [astro-ph.GA] (2025) https://doi.org/10.48550/arXiv.2505.11263

[27] Ivanov, M.A. Another origin of cosmological redshifts. arXiv:astro-ph-0405083 (2004) https://doi.org/10.48550/arXiv.astro-ph/0405083

[28] Riess, A.G. et al. A comprehensive measurement of the local value of the Hubble constant with 1 km s^{-1} Mpc^{-1} uncertainty from the Hubble space telescope and the SH0ES team. ApJL **934**, L7 (2022) https://doi.org/10.3847/2041-8213/ac5c5b

[29] He, T.-Y., Yin, J.-J., Wang, Z.-Y., Han, Z.-W., Yang, R.-J. A new parametrization of Hubble parameter and Hubble tension. J. Cosmol. Astropart. Phys **09**, 028 (2024) https://doi.org/10.1088/1475-7516/2024/09/028

[30] Liu, G., J. Gao, J., Han, Y., Mu, Y., Xu, L. Coupled Dark Sector Models and Cosmological Tensions. Phys. Rev. D **109**, 103531(2024) https://doi.org/10.1103/PhysRevD.109.103531

[31] Silva, G. P. da, Cavalcanti, A. G. A more accurate and competitive estimative of H0 in intermediate redshifts. Brazilian J. Phys. **48**, 521 (2018) https://doi.org/10.1007/s13538-018-0581-9

[32] Ivanov, M.A. Different expectations about quantum gravity. 14th International Conference on Gravitation, Astrophysics and Cosmology (ICGAC14), 17 - 21 August 2020, Jhongli, Taiwan.

[33] Ivanov, M.A. Revealing the quantum origin of gravity. The workshop Witnessing Quantum Aspects of Gravity in a Lab, São Paulo, Brazil, September 23 - 27, 2024.

[34] Betoule, M., Kessler, R., Guy, J., Mosher, J. et al. Improved cosmological constraints from a joint analysis of the SDSS-II and SNLS supernova samples. Astron. Astrophys. **568**, A22 (2014) https://doi.org/10.1051/0004-6361/201423413

[35] Ivanov, M.A. Cosmological consequences of the model of low-energy quantum gravity. In *Proc. Int. Conf. Cosmology on Small Scales 2016*, 179-198, edited by M. Krizek and Yu. Dumin, Prague: Institute of Mathematics CAS. http://http://css2016.math.cas.cz/proceedingsCSS2016.pdf.

[36] Lauer, T.R., Postman, M., Weaver, H.A., Spencer, J.R. et al. New Horizons Observations of the Cosmic Optical Background, Astrophys. J. **906**, 77 (2021) https://doi.org/10.3847/1538-4357/abc881

[37] Suzuki, N., Rubin,D., Lidman, C., Aldering, G., Amanullah,R., Barbary, K., ... & Supernova Cosmology Project. The Hubble Space Telescope Cluster Supernova Survey: V. Improving the Dark Energy Constraints Above $z > 1$ and Building an Early-Type-Hosted Supernova Sample. Astrophys. J. **746**, 85 (2012) https://doi.org/10.1088/0004-637X/746/1/85

[38] Wei, H. Observational Constraints on Cosmological Models with the Updated Long Gamma-Ray Bursts. J. Cosmol. Astropart. Phys. **08**, 020 (2010) https://doi.org/10.1088/1475-7516/2010/08/020

[39] Lin,H.-N., Li, X., Chang, Z. Effect of GRB spectra on the empirical luminosity correlations and the GRB Hubble diagram. Mon. Not. Roy. Astron. Soc. **459**(3), 2501-2512 (2016) https://doi.org/10.1093/mnras/stw817

[40] Lopez-Corredoira, M., Melia, F., Lusso, E., Risaliti, G. Cosmological test with the QSO Hubble diagram. Int. J. Mod. Phys. D **25**(5), 1650060 (2016) https://doi.org/10.1142/S0218271816500607

[41] Liu, A., Aguirre, J., Ali-Haimoud, Y., Alvarez, M. et al. Cosmology with the Highly Redshifted 21cm Line. arXiv:1903.06240v1 [astro-ph.CO] (2019) https://doi.org/10.48550/arXiv.1903.06240.

[42] Melia, F. The Anomalous 21-cm Absorption at High Redshifts. Eur. Phys. J. C **81**, 230 (2021) https://doi.org/10.1140/epjc/s10052-021-09029-4

[43] Ghara, R., Shaw, A. K., Zaroubi, S., Ciardi, B. et al. Probing the intergalactic medium during the Epoch of Reionization using 21 cm signal power spectra. Astron. Astrophys. **687**, A252 (2024) https://doi.org/10.1051/0004-6361/202449444

[44] Petroff, E., Hessels,J.W.T., Lorimer, D.R. Fast Radio Bursts. Astron. Astrophys. Rev. **27**, 4 (2019) https://doi.org/10.1007/s00159-019-0116-6

[45] Guo, H.-Y., Wei, H. Could Fast Radio Bursts Be Standard Candles? Phys. Lett. B **859**, 139120 (2024) https://doi.org/10.1016/j.physletb.2024.139120

[46] Fortunato, J.A.S., Hipolito-Ricaldi, W.S., dos Santos, M.V. Cosmography from well-localized Fast Radio Bursts. Mon. Not. Roy. Astron. Soc. **526**(2), 17731782 (2023) https://doi.org/10.1093/mnras/stad2856

[47] Ivanov, M.A. Three Different Effects of the Same Quantum Nature. PoS(EPS-HEP2021)114 https://doi.org/10.22323/1.398.0114

[48] Ivanov, M.A. Galaxy number counts in a presence of the graviton background. arXiv:astro-ph/0606223v3 (2006).

[49] Cunha, J. V., Lima, J. A. S., Pires, N. Deflationary $\Lambda(t)$ cosmology: Observational expressions. Astron. Astrophys. **390**, 809 (2002) https://doi.org/10.1051/0004-6361

[50] Loh, E.D., Spillar, E.J. A Measurement of the Mass Density of the Universe. Astrophys. J. **307**, L1 (1986) https://doi.org/10.1086/184717

[51] Ivanov, M.A. Primary postulates of the standard model as consequences of the composite nature of the fundamental fermions. Nuovo Cim. **105A**, 77 (1992) https://doi.org/10.1007/BF02730740

[52] Abbott, B.P., Abbott, R., Abbott, T.D., Abernathy, M.R., Acernese, F., Ackley, K., Adams, C., Adams, T., Addesso, P. et al. (LIGO Scientific Collaboration and Virgo Collaboration). GW150914: The Advanced LIGO Detectors in the Era of First Discoveries. Astrophys. J. Lett. **116**, 131103 (2016) https://doi.org/10.1103/PhysRevLett.116.131103

[53] Cahillane, C., Mansell, G. Review of the Advanced LIGO Gravitational Wave Observatories Leading to Observing Run Four. Galaxies **10**(1), 36 (2022) https://doi.org/10.3390/galaxies10010036

[54] Ivanov, M.A. The quantum nature of gravity seen in cosmological observations. https://vixra.org/pdf/2111.0033v2.pdf (2021).